The photovoltaic potential of femtosecond-laser textured amorphous silicon

Meng-Ju Sher[a*], Kenneth Hammond[a], Lysander Christakis[b], Eric Mazur[a,c]
[a]Department of Physics and [c]School of Engineering and Applied Sciences, Harvard University, 9 Oxford St., Cambridge, MA 02138, USA; [b]The Cambridge School of Weston, 45 Georgian Rd. Weston, MA 02493, USA

ABSTRACT

Femtosecond laser texturing of silicon yields micrometer scale surface roughness that reduces reflection and enhances light absorption. In this work, we study the potential of using this technique to improve efficiencies of amorphous silicon-based solar cells by laser texturing thin amorphous silicon films. We use a Ti:Sapphire femtosecond laser system to texture amorphous silicon, and we also study the effect of laser texturing the substrate before depositing amorphous silicon. We report on the material properties including surface morphology, light absorption, crystallinity, as well as solar cell efficiencies before and after laser texturing.

Keywords: photovoltaic, laser texturing, light trapping, amorphous silicon

1. INTRODUCTION

Hydrogenated amorphous silicon (a-Si) solar cells have several advantages over other photovoltaic materials because of strong light absorption and low processing temperature, allowing reduced material usage on low cost substrates [1]. The absorption coefficient of a-Si is higher than crystalline Si due to the lack of long-range order which reduces the momentum conservation requirement, but the disorder also causes a high concentration of defects, limiting the efficiency of charge carrier extraction. The trade-off between charge carrier extraction and optical absorption leads to devices with thin layers of a-Si combined with a light-trapping design. Moreover, defects form when a-Si is exposed to sunlight (Staebler-Wronski effect) [2], and the stabilized, light-soaked efficiency reduces by at least 10% relative to a cell's initial performance [3, 4]. In this paper, we explore treating a-Si with femtosecond laser (fs-laser) pulses to modify the crystallinity as well as the surface morphology for enhanced light absorption, and we study the effect of laser treatment on solar cell performance.

Common light trapping designs for a-Si solar cells utilize randomly textured substrates, plasmonic scattering structures [5-7], or textured transparent top contact [8, 9]. Femtosecond-laser irradiation of silicon results in semi-periodic surface textures that have periodicity on the order of the laser wavelength (800 nm in this study) [10]. Surface textures with sizes slightly smaller than the wavelength of light are ideal for diffracting incident light into shallow angles and enhance the optical path length [11]. Efficient light trapping surfaces that approaches the Lambertian limit have been demonstrated by fs-laser processing; moreover, the size of the texture can be tuned and applied to thin-film material regardless of the crystallinity [12, 13].

Compared to a-Si, nanocrystalline silicon (nc-Si) has larger carrier mobility and higher stability [14]. Solar cells fabricated with nc-Si have higher stabilized efficiency. Nanocrystalline silicon is normally fabricated under carefully controlled deposition condition [15, 16]. On the other hand, it has been demonstrated that treating a-Si with fs-laser pulses anneals and transforms a-Si into nc-Si [14, 17]. Therefore, it is promising to process a-Si solar cells with fs-laser pulses, transforming both the surface morphology and crystallinity for enhanced light absorption and material stability.

2. EXPERIMENTAL

In this paper, we use an *n-i-p* structure for the solar cell design [18], and we increase the absorption with two different methods. (a) We perform laser texturing directly on 2-μm thick hydrogenated a-Si deposited via plasma-enhanced chemical vapor deposition (PECVD). (b) We perform laser texturing on the substrate prior to a-Si deposition. The schematics of the two devices and a reference cell are illustrated in Figure 1. To simplify the fabrication process, we use

* sher@physics.harvard.edu

Laser-based Micro- and Nanopackaging and Assembly VII, edited by
Udo Klotzbach, Yongfeng Lu, Kunihiko Washio, Proc. of SPIE Vol. 8608, 86080R
 · doi: 10.1117/12.2005451

a degenerately doped silicon (p-type, 0.01 Ω·cm) not only as the substrate but also as the bottom conductive contact and the back reflector. We discuss later in the paper on how the substrate adds to series resistance and hence reduces the photovoltaic efficiency.

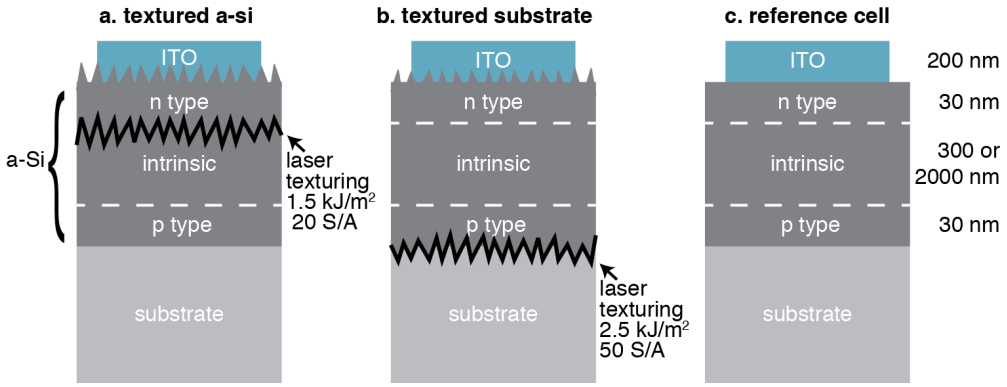

Figure 1: sample schematics. (a) laser-textured a-Si. The n-type a-Si is deposited after laser treatment on a 2-µm intrinsic layer. (b) laser-textured substrate with a-Si *n-i-p* layers deposited after the laser treatment. (c) reference cell structure. The intrinsic layer is either 300 nm or 2 µm. In all cases, the p-type and n-type a-Si layers are both 30 nm, and the ITO transparent conductive contact is 200 nm.

For laser-textured a-Si, the substrate is first solvent cleaned and then dipped in 5% hydrofluoric acid for 60 s to remove surface oxide. The wafer is then transferred to the PECVD chamber, where 30 nm of p-type a-Si is deposited, followed by a 2-µm intrinsic a-Si deposition, both at 200 ºC. The intrinsic layer is thick since subsequent laser texturing removes material through ablation. We then laser-treat the sample before depositing the final n-type a-Si layer (30 nm at 200 ºC). The laser treatment is carried out in a hydrogen ambient environment (pressure = 6.6×10^4 Pa) using a Ti:Sapphire amplified laser system (center wavelength 800 nm, pulse duration 80 fs). We use a set of scanning mirrors to process several 1×1 cm^2 squares, and, on average, 20 laser pulses were delivered to every surface of the sample. The average number of laser pulses on a given spot is referred to as "shots per area (S/A)." We optimized the overlapping of the laser pulse and the fluence (energy density F = 1.5 kJ/m^2) to produce efficient light trapping surface textures without penetrating through the 2-µm intrinsic layer.

For the cell with the laser-textured substrate (Fig. 1(b)), we perform the laser treatment first on the substrate and then deposit a-Si *n-i-p* layers (30/300/30 nm). Compared to direct texturing on a-Si, since there is no restriction on the processing thickness, we use a fluence of 2.5 kJ/m^2 and 50 shots per area.

We also fabricate reference cells for comparison. Due to the variability of sample performance from batch to batch, such as the exact thickness of the thin film deposited, we always fabricate reference cells on the same substrate as the textured cells and under identical conditions. Two types of reference cells are fabricated; both are *n-i-p* layers of a-Si, but with different intrinsic a-Si thickness: 300 and 2000 nm.

Finally, we sputter indium tin oxide (ITO, 200 nm, sheet resistance 30 Ω/□) on all the samples to form a transparent conductive top contact. The active area (0.38 cm^2) is defined by the circular shadow mask for the ITO deposition. We measure the current-bias (*I–V*) curve of each device under dark and illuminated conditions (AM1.5 spectrum with a solar simulator). Samples are also characterized using scanning electron microscopy, Raman scattering spectroscopy, and absorption measurements using a UV-VIS-FTIR spectrophotometer equipped with an integrating sphere.

3. RESULTS

Representative images of the surface of the samples are shown in Figure 2. Laser-textured a-Si samples have irregular surface features that are smaller than the textured substrate samples, which have semi-periodic surface textures. We choose the laser parameters for textured a-Si samples to ensure laser texturing doesn't penetrate the a-Si layer, which is only 2 µm. The laser-material interaction is significantly different comparing laser processing of a-Si and of crystalline Si (the substrate). Under the same fabrication conditions (1.5 kJ/m^2, 20 S/A), no surface texturing occurs on the substrate. We increased both the fluence (2.5 kJ/m^2) and the number of overlapping laser pulses (50 S/A). However, the fluence and shots per area cannot be too large, otherwise a-Si deposition is not uniform on the textured substrate.

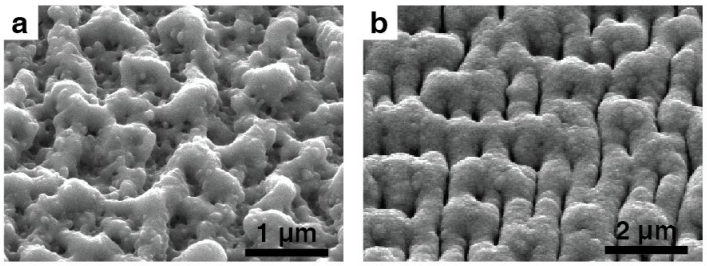

Figure 2: 45º scanning electron micrographs of the samples before ITO deposition. (a) laser-textured a-Si and (b) laser-textured substrate with a-Si *n-i-p* layers deposited on top.

Figure 3 shows the illuminated current-bias characteristics of each type of solar cell. Table 1 summarizes the best solar cell fabricated in each set of experiments. A planar a-Si solar cell should have an intrinsic layer with thickness less than 300 nm to ensure efficient carrier extraction through the amorphous material [6, 18]. The reference cell with a 300-nm intrinsic layer (Reference a1) has an efficiency of 1.89%, and the efficiencies of the laser-textured a-Si solar cells are an order of magnitude lower than the reference cells. Reference cell a2 is 2-µm thick, and the efficiency is 0.6%, smaller than Reference a1, due to the reduction in the short circuit current density (J_{SC}) from the inefficient carrier collection through the thick amorphous layer. Reference cell a2 has the same thickness as the a-Si before laser texturing (2 µm) and is 7.5 times more efficient than the textured solar cell, indicating laser processing was not effective. After laser texturing, the open circuit voltage (V_{OC}) drops from 0.82 V to 0.54 V. The drop in V_{OC} could either due to increasing shunting or due to crystallized Si (the band gap of crystalline Si is smaller than amorphous Si, resulting in a reduction of V_{OC}). On the other hand, if laser texturing is effective, J_{SC} should increase since more light is absorbed. J_{SC} of the textured a-Si solar cell, however, is much lower than both of the reference cells. This reduction in J_{SC} could be due to increased recombination at the surface or from laser-induced defects.

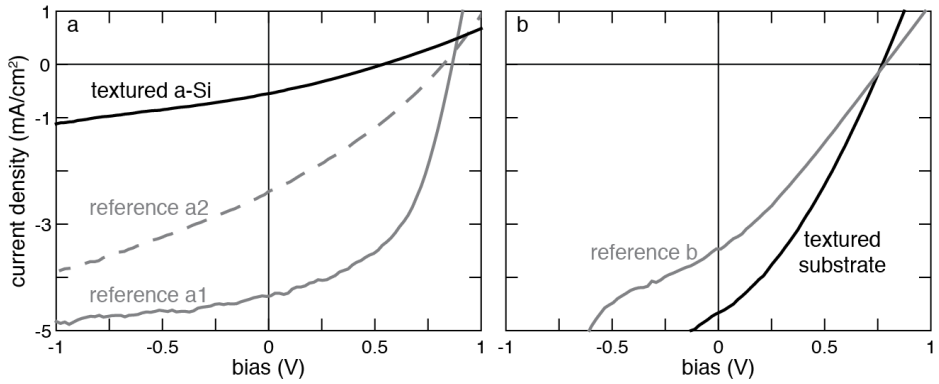

Figure 3: illuminated *I–V* curves of solar cells. (a) laser-textured a-Si solar cell (black) plotted together with two reference cells. The intrinsic a-Si thickness is 300 nm for Reference a1 (gray solid line) and is 2000 nm for Reference a2 (gray dash line). (b) solar cell on a laser-textured substrate (black) and reference b (gray) that was fabricated on the same substrate under the same condition.

Table 1: illuminated I-V data

Sample	Efficiency (%)	J_{SC} (mA/cm^2)	V_{OC} (V)	Fill factor
Textured a-Si (a)	0.08	0.55	0.54	0.28
Reference a1 (300nm)	1.89	4.37	0.86	0.50
Reference a2 (2000nm)	0.60	2.39	0.82	0.31
Textured substrate (b)	1.18	4.68	0.78	0.32
Reference b (300nm)	0.78	3.46	0.78	0.29

Figure 3b compares the solar cells fabricated on top of the textured substrate and Reference b. To avoid the variability mentioned above, Reference b is fabricated on the same chip as the solar cells on the textured substrate. The V_{OC} is the same but the J_{SC} is improved by 35 %. As a result the efficiency increases by 0.4% absolute. We note that Reference b is not as efficient as Reference a1, which ideally should be the same. Due to practical reasons, the exact same a-Si

deposition parameter was not feasible when this set of textured substrate and reference cells was fabricated, so the deposition conditions were slightly different between the two reference cells (a1 and b).

Figure 4 shows that for the laser-textured a-Si sample, the absorption increases, and the laser processing also crystallizes silicon. To perform optical absorption measurements, we deposit a-Si on a transparent glass and laser-texture the sample with the parameters described in the experimental section. We measure the light transmittance (T) and reflectance (R) and calculate absorptance as $A = 100 - T - R$ (%). The fringes in the absorptance curves in the near infrared range are because of multiple reflections of light at both the front and back surface of the thin film, which interfere constructively or destructively depending on both the thickness of the a-Si film and the wavelength of the incident light [19]. After laser texturing, the above band gap light absorption increases by 20% absolute and the absorption edge is shifted toward longer wavelength. Furthermore, before laser texturing, the Raman spectrum of the reference sample shows the signature a-Si Raman shift at 480 cm^{-1} [14]. After laser texturing, a sharp Raman peak at 520 cm^{-1} indicates that some amorphous silicon is transformed into crystalline silicon.

It is not easy to quantify the amount of absorption enhancement present in the laser-textured substrate sample since the silicon substrate is not transparent and thus transmittance measurements cannot be performed. In the visible light range, the reflectance of the surface is less than 20%, compared to a reflectance of about 40% for planar a-Si. Since no laser treatment is performed on the deposited a-Si, we do not expect the material crystallinity to change.

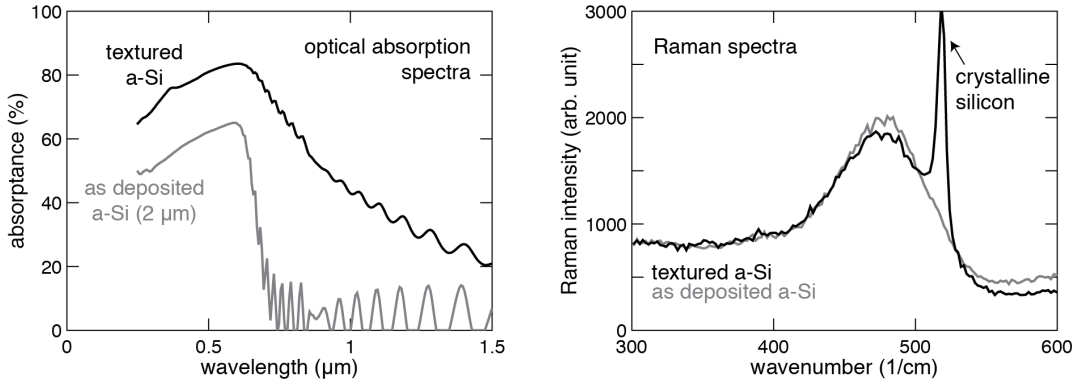

Figure 4: Optical absorption spectra (left) and Raman spectra (right) of laser-textured a-Si and a reference sample.

4. DISCUSSION

The solar cells fabricated from laser-textured a-Si are an order of magnitude less efficient than the reference cells, while a-Si solar cells on top of the laser-textured substrate increase the short circuit current and hence the efficiency. Within the parameters presented in this paper, fs-laser texturing and crystallization of a-Si directly for photovoltaic applications does not work as well as enhancing the light absorption by using a fs-laser textured substrate. We discuss possible reasons for low efficiencies after laser treating a-Si and suggest future directions for enhancing light absorption using laser treated substrates.

This experiment is a proof-of-principle study; therefore, many fabrication parameters are not optimized and the efficiencies of the cells in this study are lower than what is commonly achieved [1]. For example, we chose silicon as a substrate to ensure good a-Si adhesion for CVD deposition, but this substrate is more resistive and less reflective than common back contacts. Furthermore, the sputtered ITO is also more resistive than the desired transparent front contact [18]. This is likely due to the fact that the oxygen content and the substrate temperature are not optimized during sputtering. Both the front and back contacts introduce resistive loss and lower the overall efficiency. Since the substrate and the ITO contact are the same across all of our samples, though, we can still compare the performance of different samples with their reference cells.

We now discuss possible reasons for the efficiency reduction after laser texturing the a-Si. First, we observe the formation of pinholes after laser irradiation. We suspect that the hydrogen from the hydrogenated a-Si outgases quickly when the sample is heated by the laser, leaving behind pinholes. Starting with a-Si film that has lower hydrogen concentration could avoid formation of pinholes that degrade the material quality, but our experimental setup does not

allow changing the concentration of hydrogen in the a-Si film. We observe fewer pinholes when using laser fluences higher than 1.5 kJ/m^2, so there could be better laser parameters that avoid pinhole formation. Secondly, as the surface textures develop, the local fluence of the laser pulses is no longer uniform across the rough surface, and it is possible that this causes heating and diffusion in the p-type layer underneath. As a result, laser irradiation could affect the interface between the p-type and the intrinsic a-Si. Future work will focus on fine tuning the laser parameters to ensure that laser texturing removes enough excessive a-Si for texturing but does not over-texture and affect the p-type layer underneath.

Since currently we cannot achieve higher efficiencies by using fs-laser treatment to both enhance absorption and to crystallize silicon, we decouple the surface texturing and laser irradiation of a-Si by performing laser texturing on the substrate. In principle, if the thickness of the a-Si solar cell is reduced, the Staebler-Wronski effect will also be reduced [1, 5]. We show increased efficiency when the laser irradiation is no longer directly on a-Si. Moreover, fs-laser texturing can be achieved on a wide variety of substrates [20-22], so this experiment shows that we can use the laser texturing technique to enhance light absorption for a-Si solar cells. The thickness of the a-Si solar cells can be further optimized for efficient carrier collection and reduced light-soaked efficiency reduction. Furthermore, investigating the use of fs-laser treatment to texture different substrates and optimizing the surface morphology for light trapping should also improve the efficiency.

We demonstrated that laser texturing the substrate is a feasible method for improving light absorption. The semi-periodic textured surface created by fs-laser processing is effective for anti-reflection and light trapping. In the future, it may also be possible to use these surface textures for template stripping [23, 24] or nanoimprint lithography [5] to replicate these surface structures quickly and large scales.

5. CONCLUSION

In conclusion, we apply fs-laser processing techniques to texture and crystallize a-Si for photovoltaic applications. While the absorption and crystallinity of fs-laser processed a-Si improves, the overall cell efficiency does not increase, due to irradiation-induced damage such as pinhole formation. On the other hand, light absorption can be improved by fabricating a-Si solar cells on laser-textured substrates, which improves both the short circuit current and the efficiency. Future work on tuning the laser processing parameters for texturing a-Si with lower hydrogen content as well as laser texturing ZnO or glass (which are common back contacts and substrates for a-Si solar cells) could yield fruitful results.

ACKNOWLEDGMENTS

Several people contributed to this work. M. S. conceived of the experiment; M.S., K.H. and L.C. fabricated the samples and carried out device characterization. E.M. supervised the research. The authors would like to acknowledge Benjamin Franta for his assistance editing the manuscript. The research described in this paper was supported by The National Science Foundation under contracts DMR-0934480. This work was performed in part at the Center for Nanoscale Systems (CNS), a member of the National Nanotechnology Infrastructure Network (NNIN), which is supported by the National Science Foundation under NSF award no. ECS-0335765. CNS is part of Harvard University.

REFERENCES

[1] Rech, B. and H. Wagner, "Potential of amorphous silicon for solar cells," Applied Physics a-Materials Science & Processing 69(2), 155-167 (1999).

[2] Fritzsche, H., "Development in understanding and controlling the Staebler-Wronski effect in a-Si : H," Ann. Rev. Mater. Res. 31, 47-79 (2001).

[3] Meier, J., et al., "Potential of amorphous and microcrystalline silicon solar cells," Thin Solid Films 451, 518-524 (2004).

[4] Matsui, T., et al., "Amorphous-Silicon-Based Thin-Film Solar Cells Exhibiting Low Light-Induced Degradation," Japanese Journal of Applied Physics 51(10), (2012).

[5] Ferry, V.E., et al., "Light trapping in ultrathin plasmonic solar cells," Opt. Express 18(13), A237-A245 (2010).

[6] Derkacs, D., et al., "Improved performance of amorphous silicon solar cells via scattering from surface plasmon polaritons in nearby metallic nanoparticles," Applied Physics Letters 89(9), (2006).

[7] Ho, C.I., et al., "Plasmonic multilayer nanoparticles enhanced photocurrent in thin film hydrogenated amorphous silicon solar cells," Journal of Applied Physics 112(2), (2012).
[8] Hsu, C.M., et al., "High-Efficiency Amorphous Silicon Solar Cell on a Periodic Nanocone Back Reflector," Adv. Energy Mater. 2(6), 628-633 (2012).
[9] Eisele, C., C.E. Nebel, and M. Stutzmann, "Periodic light coupler gratings in amorphous thin film solar cells," Journal of Applied Physics 89(12), 7722-7726 (2001).
[10] Tull, B.R., et al., "Silicon surface morphologies after femtosecond laser irradiation," Mrs Bulletin 31(8), 626-633 (2006).
[11] Han, S.E. and G. Chen, "Toward the Lambertian Limit of Light Trapping in Thin Nanostructured Silicon Solar Cells," Nano Letters 10(11), 4692-4696 (2010).
[12] Iyengar, V.V., B.K. Nayak, and M.C. Gupta, "Optical properties of silicon light trapping structures for photovoltaics," Solar Energy Materials and Solar Cells 94(12), 2251-2257 (2010).
[13] Lee, B.G., et al. *Light trapping for thin silicon solar cells by femtosecond laser texturing*. in *Photovoltaic Specialists Conference (PVSC), 2012 38th IEEE*. 2012.
[14] Emelyanov, A.V., et al., "Effect of the femtosecond laser treatment of hydrogenated amorphous silicon films on their structural, optical, and photoelectric properties," Semiconductors 46(6), 749-754 (2012).
[15] Mai, Y., et al., "Microcrystalline silicon solar cells deposited at high rates," Journal of Applied Physics 97(11), (2005).
[16] Pearce, J.M., et al., "Optimization of open circuit voltage in amorphous silicon solar cells with mixed-phase (amorphous + nanocrystalline) p-type contacts of low nanocrystalline content," Journal of Applied Physics 101(11), 114301-7 (2007).
[17] Shieh, J.-M., et al., "Near-infrared femtosecond laser-induced crystallization of amorphous silicon," Applied Physics Letters 85(7), 1232-1234 (2004).
[18] Razykov, T.M., et al., "Solar photovoltaic electricity: Current status and future prospects," Solar Energy 85(8), 1580-1608 (2011).
[19] The transmission measurement is performed at normal incidence and reflection measurement is performed at a small angle offset (8º) in order to capture the reflected light. When calculating absorption from transmission and reflection data, the fringes should cancel out if the samples are perfectly aligned. These fringes are very sensitive to the measurement angle and in our setup T and R are performed at slightly different angle, so after computing the absorptance, the fringes do not cancel out perfectly.
[20] Shen, M.Y., "Nanostructuring Solid surfaces With Femtosecond Laser Irradiations for Applications," Modern Physics Letters B 24(3), 257-269 (2010).
[21] Dufft, D., et al., "Femtosecond laser-induced periodic surface structures revisited: A comparative study on ZnO," Journal of Applied Physics 105(3), 034908-9 (2009).
[22] Kumar Das, S., et al., "Femtosecond-laser-induced quasiperiodic nanostructures on TiO[sub 2] surfaces," Journal of Applied Physics 105(8), 084912-5 (2009).
[23] Zhou, W. and T.W. Odom, "Tunable subradiant lattice plasmons by out-of-plane dipolar interactions," Nat. Nanotechnol. 6(7), 423-427 (2011).
[24] Nagpal, P., et al., "Ultrasmooth Patterned Metals for Plasmonics and Metamaterials," Science 325(5940), 594-597 (2009).